Eco-geomorphic implications of hillslope aspect: Inferences from analysis of landscape morphology in central New Mexico

Erkan Istanbulluoglu,[1,2] Omer Yetemen,[1] Enrique R. Vivoni,[3] Hugo A. Gutiérrez-Jurado,[3] and Rafael L. Bras[4]

Received 29 April 2008; accepted 17 May 2008; published 31 July 2008.

[1] We investigate the influence of hillslope aspect on landscape morphology in central New Mexico, where differences in soils, vegetation, and landforms are observed between mesic north-facing and xeric south-facing slopes. Slope–area and curvature–area relations, derived from a Digital Elevation Model (DEM), are used to characterize the opposing hillslope morphologies. In all geologies and elevation ranges studied, topographic data reveal significantly steeper slopes in north-facing aspects, and shallower slopes in south-facing aspects. North-facing slope curvatures are also greater than south-facing curvatures. Using a conceptual slope-area model, we suggest that for a given drainage area, steeper north-facing slopes imply lower soil erodibility. We argue that this interpretation, consistent with recent views of ecosystem control on semiarid erosion rates, shows the influence hillslope aspect on topography and its associated vegetation communities. Observed valley asymmetry in the region reinforces this concept and suggests a long-term legacy of aspect-modulated ecogeomorphic processes. **Citation:** Istanbulluoglu, E., O. Yetemen, E. R. Vivoni, H. A. Gutiérrez-Jurado, and R. L. Bras (2008), Eco-geomorphic implications of hillslope aspect: Inferences from analysis of landscape morphology in central New Mexico, *Geophys. Res. Lett.*, *35*, L14403, doi:10.1029/2008GL034477.

1. Introduction

[2] Hillslope aspect has important effects on soil and vegetation development in many climates [*Carson and Kirkby*, 1972]. In addition to soils and vegetation, there is growing evidence for aspect control on hillslope morphology [*Walker*, 1948; *Melton*, 1960; *Carson and Kirkby*, 1972; *McMahon*, 1998]. This is expected because soil and vegetation properties [*Roering et al.*, 2004; *Istanbulluoglu and Bras*, 2005] and local microclimate and hydrological conditions influence sediment transport [*Gutiérrez-Jurado et al.*, 2007].

[3] In western Wyoming, for example, *Walker* [1948] observed steeper and straighter slope profiles on forested north-facing hillslopes, and less steep, and more concave slope profiles on grass-covered south-facing slopes. Similar contrasts were reported in other east-west flowing valleys in Wyoming [*Melton*, 1960], in the Mancos Shales rim of southwest United States (US) [*Carson and Kirkby*, 1972], and the foothills near Denver, Colorado, US [*Brandon and Shown*, 1990]. These were often attributed to much greater rates of surface wash on the less vegetated south-facing slopes, and soil creep on the vegetated north-facing slopes [*Carson and Kirkby*, 1972].

[4] The aforementioned studies suggest a close tie between ecological and geomorphologic processes leading to differences in north and south facing slope morphologies. However, a mechanistic interpretation of such observations, critical for landscape evolution modeling, has not been adequately described. We examine topography in central New Mexico, where north- and south-facing slopes show differences in soil and vegetation types. Slope-area and curvature-area relations are used to interpret the influence of aspect on landscape evolution, in connection to regional climate variations and vegetation change.

2. Background

2.1. Slope-Area Relation

[5] A well-known empirical observation in geomorphology relates local landscape slope, S, and its drainage area, A, according to a power-law:

$$S = k \cdot A^{\theta} \tag{1}$$

where k is a constant and θ is a scaling exponent, that is the gradient (degree of steepness) of the slope-area relation in a log-log plot ($\log(S) = \log(k) + \theta\log(A)$). Empirically, θ is positive in rounded convex ridges where diffusive sediment transport (e.g., soil creep, rain splash, bioturbation) is dominant, and negative in concave valleys and channels where fluvial (advective) sediment transport erodes the landscape [*Tarboton et al.*, 1992].

[6] Theoretically, both k and θ have been related to landscape-scale denudation rate and the form of sediment transport [*Tarboton et al.*, 1992]. In basins with abundant supply of sediment, long term average sediment transport rate at a given point on the landscape, Q_s, can be expressed as:

$$Q_s = KA^m S^n, \tag{2}$$

where K is an erodibility parameter, and m and n are empirical exponents.

[7] If the long-term denudation rate (D) is equal everywhere in the basin, $Q_s = D\,A$, then S in (2) adjusts to A such that

[1]School of Natural Resources, University of Nebraska at Lincoln, Lincoln, Nebraska, USA.
[2]Also at Department of Biological Systems Engineering, University of Nebraska at Lincoln, Lincoln, Nebraska, USA.
[3]Department of Earth and Environmental Science, New Mexico Institute of Mining and Technology, Socorro, New Mexico, USA.
[4]Department of Civil and Environmental Engineering, Massachusetts Institute of Technology, Cambridge, Massachusetts, USA.

0094-8276/08/2008GL034477

sediment transport capacity is just equal to total incoming sediment flux, leading to the following expressions:

$$k = \left(\frac{D}{K}\right)^{\frac{1}{n}} \tag{3a}$$

$$\theta = \frac{1-m}{n} \tag{3b}$$

For diffusive sediment transport, m is 0, and therefore the gradient in the slope-area relation is positive ($\theta > 0$) on ridges with negligible fluvial sediment transport. For fluvial sediment transport, both m and $n > 1$, with which (3b) predicts $\theta < 0$, leading to a negative gradient in the slope-area relation of valleys and channels. Differences in m and n in unchanneled versus channeled flows may also introduce a change in θ as valley area grows [*Ijjasz-Vasquez and Bras*, 1995].

2.2. Curvature-Area Relation

[8] Landscape curvature (i.e. Laplacian of elevation z, $\nabla^2 z$) is another useful measure for the interpretation of dominant sediment transport processes on the landscape. Total curvature is defined as the sum of both plan ($\partial^2 z/\partial x^2$) and profile ($\partial^2 z/\partial y^2$) curvatures:

$$\nabla^2 z = \left(\frac{\partial^2 z}{\partial x^2} + \frac{\partial^2 z}{\partial y^2}\right). \tag{4}$$

Plan curvature represents the degree of divergence or convergence perpendicular to flow direction. Profile curvature represents the convexity or concavity along the flow direction. In general terms, divergent-convex landforms ($\nabla^2 z < 0$) are formed by hillslope diffusion, while concave-convergent landforms ($\nabla^2 z > 0$) result from fluvial sediment transport.

3. Field Site and Response to Geomorphically Significant Flood

[9] The slope-area and curvature-area relations described above are examined in several small basins (1.8 km^2–12 km^2 in area), located in the northwestern corner of the Sevilleta National Wildlife Refuge (SNWR) in central New Mexico (Figure 1). Regional climate is semiarid with ~250 mm of mean annual precipitation comprising high-intensity summer monsoon storms and low-intensity winter precipitation.

[10] Geology of the study region is characterized by two units of the Sante Fe Group: the early Pliocene to middle Pleistocene Sierra Ladrones Formation (SLF), consisting of alluvial fan, piedmont slope, floodplain and axial stream deposits; and early to late Miocene Popotosa Formation (PF). PF is the deepest unit within the Santa Fe Group, and is typically overlain by SLF [*Green and Jones*, 1997]. Topography of the region is composed of slightly steeper and planar north-facing slopes (Figure 1c); and highly dissected south-facing slopes (Figure 1d).

[11] In the study region, the north-facing slopes are typically savanna ecosystems with one-seed Juniper (*Juniperus monosperma*) and dense black grama (*Bouteloua eriopoda*). The south-facing slopes are xeric ecosystems comprised primarily of creosotebush (*Larrera tridentata*) and sparser fluff grass (*Erioneuron pulchellum*). In general, surface sediments are characterized by desert pavements on the upper hilltops and coarse sandy matrices in valleys in the SLF (Figure 1b, see star for location) [*McMahon*, 1998; *Gutiérrez-Jurado et al.*, 2006]. Compared to south-facing slopes, north-facing soils typically contain higher fractions of silt, clay and organic matter as well as higher stages of $CaCO_3$ layer development. This is often related to greater vegetation biomass on north facing slopes that enhance the influx of material (e.g., trapping of aeolian dust and particles) and organic matter into the soil; and the precipitation of $CaCO_3$ [*Gutiérrez-Jurado et al.*, 2006].

[12] Recently, *Gutiérrez-Jurado et al.* [2007] documented the ecohydrological response of opposing aspects in the SLF to a large storm event. The north-facing juniper-grass savanna retained significant moisture. In contrast, interconnected bare patches on south-facing slope retained less moisture, produced the majority of the basin runoff, and caused rill erosion. These observations reinforce the conceptual model of *Wilcox et al.* [2003] for ecosystem controls on semiarid runoff and erosion rates. The north-facing slope shows a typical resource conserving behavior while the south-facing slope exhibits a leaky behavior [*Gutiérrez-Jurado et al.*, 2007]. Although these ecohydrological differences have only been recorded for the SLF, we believe the same holds true for the PF, as they have similar soil, vegetation, and climate characteristics.

[13] To examine the influence of aspect on relatively homogenous surface conditions, we select basins that are individually underlain by the same lithology and have relatively small elevation gradients. Four basins are selected on the Upper SLF (Qts/Qtf: geological classification code used in the regional digital geology map [*Green and Jones*, 1997], Figure 1a); three at a higher elevation range (1711 m and 1920 m), and one at a lower elevation range (1567 m and 1711 m). Three other small basins are selected on PF (Tp), all between 1628 m and 1789 m elevation (Figure 1a). The role of aspect on heterogeneous landforms is also investigated in a basin composed of the piedmont-slope facies of the SLF in the headwaters (Qps), Tp and Qts/Qtf in the middle, and valley border alluvium (Qp) near the outlet, with an elevation range of 1566 m–1907 m (Figure 1a).

[14] For topographic analysis, a 10-m DEM of the SNWR derived from interferometric synthetic aperture radar (IFSAR) is used. At each DEM grid cell, drainage area, slope, and aspect are derived using standard GIS algorithms. In the analysis, all NE, NW and N bearings are identified as north-facing pixels, similarly S, SW and SE bearings are identified as south-facing.

4. Results and Discussion

4.1. Slope-Area and Curvature-Area Relations

[15] We present the slope-area and curvature-area relations of the basins in the SLF (lower basin Figures 2a and 2c; higher basin Figures 2b and 2d); the PF (Figures 2e and 2g), and the heterogeneous lithology (Figures 2f and 2h). To facilitate comparisons, average local slope and curvature, calculated for pixels grouped according to the values of

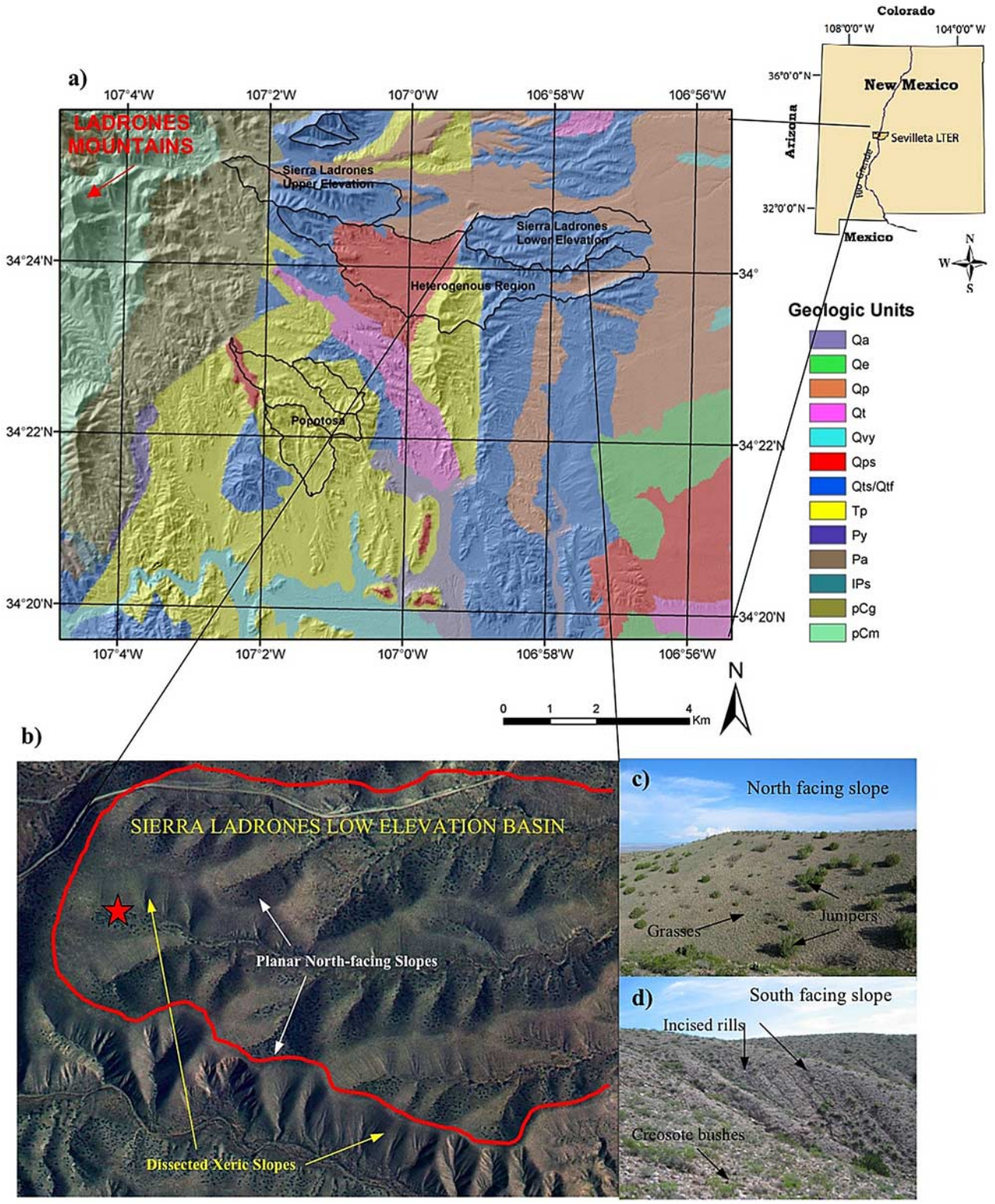

Figure 1. (a) Study basins in the SNWR in Sevilleta, NM, shown on regional geology map. (b) 2-m aerial orthophoto of parts of the SL low elevation basin. Star indicates monitoring sites of *Gutiérrez-Jurado et al.* [2007]. (c) Planar north-facing slope with juniper-grass savanna ecosystem. (d) Converging south-facing slope dominated by creosotebush and incised rills.

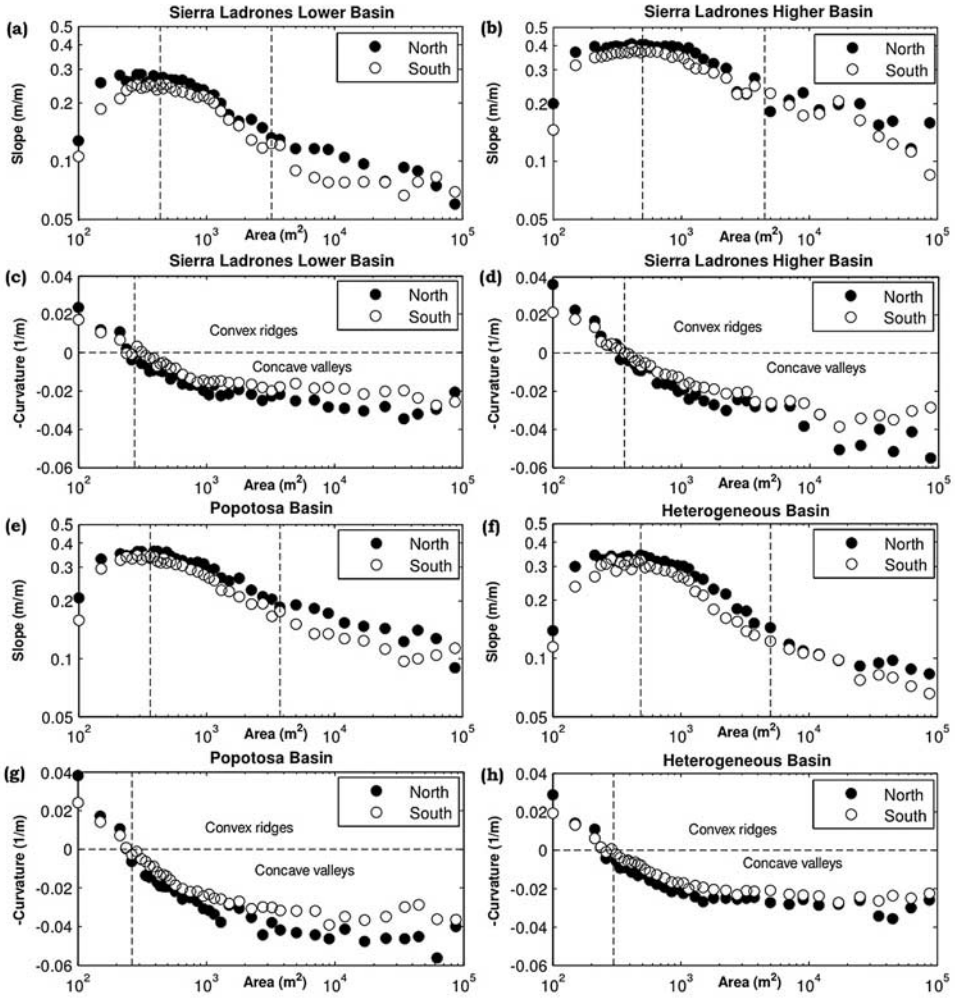

Figure 2. Slope – area and curvature – area plots of north- and south-facing slopes of the basins on the SL lower elevation (a, c) and higher elevation (b, d); PF (e, g); and heterogeneous lithology (f, h). Regions I, II, and III in the slope-area domain are based on south-facing slope trends.

contributing area, are plotted. The analyses are limited to small hillslopes (<0.1 km^2) within the selected basins, as larger areas mostly correspond to east-flowing channels.

[16] In Figure 2, three distinct slope-area scaling regimes (regions I, II and III) are identified. Plotted data points are sparse in region III as only 8% of our data falls in that region. In region I, the slope-area scaling has a positive gradient ($\theta > 0$). In region II, the gradient turns negative, gradually increases, and attains a high value as area grows. In region III, the gradient is negative, but lower than region II. In all plots, dashed vertical lines indicate region boundaries for south- facing slopes.

[17] Change in the sign of θ from region I to II corresponds to the switch between convex diffusion-dominated ridges to concave valleys where episodic rill erosion takes place (e.g., Figure 1d). In the curvature-area figure, this transition is manifested by a change in the sign of curvature from negative to positive values, though with a smaller area (Figures 2c, 2d, 2g, and 2h). This suggests that on average, concave valleys form slightly downslope on the landscape where valley convergence begins. The downward-curved portion of region II is followed by a negative slope-area trend representing regions of high valley concavity and increasing valley convergence. In all basins, region III corresponds to the main channel network where the convergence remains high (Figures 2c, 2d, 2g, and 2h).

[18] Average local slopes are slightly larger in north-facing slopes than south-facing slopes (Figures 2a, 2b, 2e, and 2f) across all geologies and elevation ranges. Based on t-tests, 71% and 61% of the opposing average slopes have different means at $\alpha = 0.05$ and $\alpha = 0.01$ significance levels respectively. Compared to south-facing slopes, north-facing aspects show both slightly higher positive curvature on ridges and higher negative curvature in valleys (Figures 2c, 2d, 2g, and 2h). The differences are statistically significant in 61% ($\alpha = 0.05$) and 45% ($\alpha = 0.01$) of the plotted average curvature data.

[19] Slope-area relations show some disparities, especially in the SLF basins. Slopes are steeper in the higher elevation SLF basin (Figure 2b) than its lower elevation counterpart (Figure 2a). Climate and vegetation patterns are similar in both basins. Arguably, observed steeper slopes might be attributed to an increase in lithological resistance with elevation [e.g., *Hack and Goodlett*, 1960].

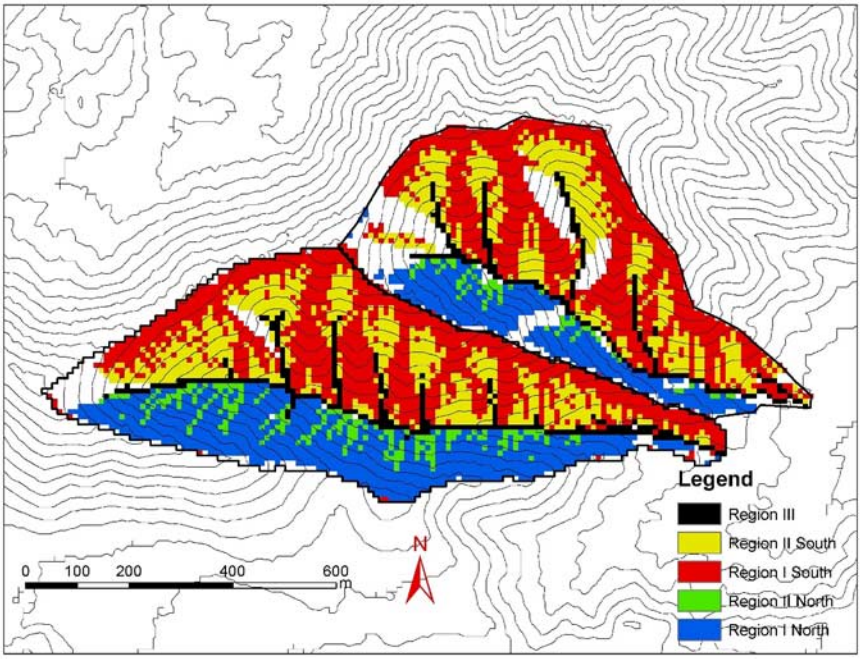

Figure 3. The three slope-area regions identified for north- and south-facing aspects on the DEM of the SL higher elevation basins. Region boundaries are obtained from Figure 2b. The upper limit of region I are 500 m^2 for south- and 1100^2 for north-facing slopes. Region III is mapped for all basins areas greater than 2400 m^2 regardless of aspect. East and west facing slopes are not included in the analysis.

[20] The north facing slopes of the SLF show a flat region between ~200 m^2 and ~600 m^2 (Figure 2a), and between ~300 m^2 and ~1100 m^2 (Figure 2b). On south facing slopes, the transition between positive and negative θ occurs at smaller drainage areas, and an absence of a flat region is observed. Consistent with our field observations (Figure 1c), a flat region on the slope-area relationship would imply planar slope profiles. For spatial comparison of the implications of the slope-area relationship on basin morphology, basin areas that fall within the three slope-area regions are mapped for the opposing aspects in the SLF higher elevation basin based on Figure 2b (see Figure 3). Note that in Figure 2b, region II of the north-facing slope begins with a larger drainage area. In Figure 3, region I of north-facing slopes contain mostly straight contour lines and longer slope segments, as opposed to mostly diverging contours and shorter hillslope length of south-facing slopes. Region II shows converging amphitheater-like valley morphology on south facing slopes, while valleys in steeper north-facing slopes are concave but less convergent, and often occupied by a single DEM cell. A noticeable valley asymmetry is also observed in Figure 3.

4.2. Erosion Processes and the Slope-Area Relation

[21] Observed differences in slope-area diagrams of the opposing aspects may be interpreted from the conceptual slope-area model (equation 2). In our basins, the majority of north- and south-facing slopes drain into east-west flowing main channels. In such geomorphic settings, the long-term local erosion rate in both aspects are expected to be identical, and equal to the lowering rate of the main channel. In equation 2, S is inversely proportional to K; therefore, under a constant D, steeper north-facing slopes for a given drainage area would imply a lower K. Conversely, lower south-facing slopes would imply a higher K (i.e., more active wash erosion) in order to maintain a constant D.

[22] This model-based explanation has important implications for landscape curvature. In north-facing ridges, slope steepening would also cause an increase in negative curvature such that the landscape could disperse more sediment [*Roering et al.*, 2004]. As a result, steeper north-facing slopes should develop higher valley concavity to adjust to the same base elevation, as borne out by our analysis, especially where there is pronounced valley asymmetry (Figure 3).

[23] Recent conceptual models of ecosystem controls on semiarid erosion rates suggest lower runoff and erosion from resource conserving vegetated slopes, as opposed to higher runoff and erosion from sparsely vegetated slopes or interconnected bare patches [*Wilcox et al.*, 2003]. Consistent with these views, more erodible south-facing slopes could maintain long-term erosion rates equal to base-level fall with shallower slopes, while more resistant north-facing slopes need higher slope to keep up with base-level fall. However, our interpretation raises an important question: Are the observed slope differences caused by modern aspect-induced soils and vegetation patterns, or are there relict influences in the observed patterns? The vegetation and erosion history of the region is necessary to address this question. We briefly explored this in the next section.

4.3. Holocene History of Climate, Vegetation, and Erosion

[24] The late Pleistocene (30,000–13,000 yr BP) in the southwestern US was wetter and cooler than the Holocene and present. At that time, today's desert elevations (300–

1700 m) were covered by pinon-juniper-oak woodlands, while shrubs were restricted to elevations lower than 300 m [*Betancourt et al.*, 1990; *Holmgren et al.*, 2007]. The early Holocene experienced a rapid transition to a monsoon-dominated climate leading to the migration of pinon-juniper populations in the Chihuahuan desert to higher elevations. Packrat midden records suggest that creosotebush was established in our study elevations approximately 4,000 yr BP [*Holmgren et al.*, 2007]. With shrub establishment and climate stress, pinon-juniper woodlands at low elevation were confined to wetter north-facing slopes.

[25] Under this scenario, in the second half of the Holocene, north-facing slopes became (or remained) ecologically efficient and resource conserving, while the south-facing slopes became ecologically less efficient or leaky. Consequently, it is conceivable that increased erodibility as a result of vegetation loss and enhanced runoff on south-facing slopes have led to slope reductions. In this region, high erosion rates in the late Holocene and present have been related to sparse vegetation cover [*Bierman et al.*, 2005].

[26] The observed evidence for valley asymmetry also supports this hypothesis (e.g., Figure 3), where south- and north-facing slopes correspond to 49% and 33% of all basin areas, respectively. Preferential undercutting of north-facing slopes as a result of enhanced deposition in the toe of south-facing slopes are among the causes of valley asymmetry [*Melton*, 1960; *Kirkby et al.*, 1990]. Formation of highly asymmetric slopes would require longer time scales than the late Holocene. As a result, differences in surface erodibility on the opposing hillslopes must have existed during certain periods throughout the Pleistocene, leading to differential slope adjustments.

5. Conclusions

[27] In our field sites in central New Mexico, topographic data reveal steeper slopes in mesic north-facing aspects and shallower slopes in xeric south-facing aspects. Using a conceptual slope-area model, shallower south-facing slopes are related to greater soil erodibility. Our interpretation supports recent studies of ecosystem control on semiarid erosion rates. This indicates that the observed morphologies of landforms in our field sites are in agreement with the topographic outcomes expected under current aspect-modulated erosion processes. The observed valley asymmetry not only reinforces this argument, but also indicates a legacy of aspect influence on biotic-abiotic hillslope process interactions which have been active (at least periodically) in former climates.

[28] **Acknowledgments.** This work was partly supported by NSF grant EAR-0819923 (Istanbulluoglu and Vivoni), and NASA grant NNG05GA17G (Bras and Vivoni).

References

Betancourt, J. L., T. R. Van Devender, and P. S. Martin (1990), *Packrat Middens: The Last 40,000 Years of Biotic Change*, 467 pp., Univ. of Ariz. Press, Tucson.

Bierman, P. R., J. M. Reuter, M. Pavich, A. C. Gellis, M. W. Caffee, and J. Larsen (2005), Using cosmogenic nuclides to contrast rates of erosion and sediment yield in a semiarid, arroyo-dominated landscape, Rio Puerco Basin, New Mexico, *Earth Surf. Processes Landforms*, *30*, 935–953.

Brandon, F. A., and L. M. Shown (1990), Contrasts of vegetation, soils microclimates, and geomorphic processes between north and south facing slopes on Green Mountain near Denver, Colorado, *U.S. Geol. Surv. Water Resour. Invest. Rep. 89-4094*.

Carson, M. A., and M. J. Kirkby (1972), *Hillslope Form and Process*, 475 pp., Cambridge Univ. Press, Cambridge, U.K.

Green, G. N., and G. E. Jones (1997), The digital geologic map of New Mexico in ARC/INFO format, *U.S. Geol. Surv. Open File Rep. OFR 97-0052*.

Gutiérrez-Jurado, H. A., E. R. Vivoni, J. B. J. Harrison, and H. Guan (2006), Ecohydrology of root zone water fluxes and soil development in complex semiarid rangelands, *Hydrol. Processes*, *20*, 3289–3316, doi:10.1002/hyp.6333.

Gutiérrez-Jurado, H. A., E. R. Vivoni, E. Istanbulluoglu, and R. L. Bras (2007), Ecohydrological response to a geomorphically significant flood event in a semiarid catchment with contrasting ecosystems, *Geophys. Res. Lett.*, *34*, L24S25, doi:10.1029/2007GL030994.

Hack, J. T., and J. C. Goodlett (1960), Geomorphology and forest ecology of a mountain region in the Central Appalachian, *U.S. Geol. Surv. Prof. Pap., 347*, 66 pp.

Holmgren, C. A., J. Norris, and J. L. Betancourt (2007), Inferences about winter temperatures and summer rains from the late Quaternary record of C4 perennial grasses and C3 desert shrubs in the northern Chihuahuan Desert, *J. Quaternary Sci.*, *22*, 141–161, doi:10.1002/jqs.1023.

Ijjasz-Vasquez, E. J., and R. L. Bras (1995), Scaling regimes of local slope versus contributing area in digital elevation models, *Geomorphology*, *12*, 299–311.

Istanbulluoglu, E., and R. L. Bras (2005), Vegetation-modulated landscape evolution: Effects of vegetation on landscape processes, drainage density, and topography, *J. Geophys. Res.*, *110*, F02012, doi:10.1029/2004JF000249.

Kirkby, M. J., K. Atkinson, and J. Lockwood (1990), Aspect, vegetation cover and erosion on semi-arid hillslopes, *Vegetation and Erosion*, edited by J. B. Thornes, pp. 25–39, John Wiley, Hoboken, N. J.

McMahon, D. R. (1998), Soil, landscape and vegetation interactions in a small semi-arid drainage basin: Sevilleta National Wildlife Refuge, M.S. thesis, 174 pp., New Mexico Inst. of Mining and Technol., Socorro.

Melton, M. A. (1960), Intravalley variation in slope angles related to microclimate and erosional environment, *Geol. Soc. Am. Bull.*, *71*, 133–144.

Roering, J. J., P. Almond, P. Tonkin, and J. McKean (2004), Constraining climatic controls on hillslope dynamics using a coupled model for the transport of soil and tracers: Application to loess-mantled hillslopes, South Island, New Zealand, *J. Geophys. Res.*, *109*, F01010, doi:10.1029/2003JF000034.

Tarboton, D. G., R. L. Bras, and I. Rodriguez-Iturbe (1992), A physical basis for drainage density, *Geomorphology*, *5*, 59–76.

Walker, E. H. (1948), Differential erosion on slopes of northern and southern exposure in western Wyoming (Abstract), *Geol. Soc. Am. Bull.*, *59*, 1360.

Wilcox, B. P., D. D. Breshears, and C. D. Allen (2003), Ecohydrology of a resource-conserving semiarid woodland: Effects of scale and disturbance, *Ecol. Monogr.*, *73*(2), 223–239.

R. L. Bras, Department of Civil and Environmental Engineering, Massachusetts Institute of Technology, Cambridge, MA 02139, USA.

H. A. Gutiérrez-Jurado and E. R. Vivoni, Department of Earth and Environmental Science, New Mexico Institute of Mining and Technology, Socorro, NM 87801, USA.

E. Istanbulluoglu and O. Yetemen, School of Natural Resources, University of Nebraska at Lincoln, Lincoln, NE 68588, USA. (erkan2@unl.edu)